ICAS 2016
30th Congress of the International Council of the Aeronautical Sciences
DCC, Daejeon, Korea ; September 25-30, 2016

Bifurcation Analysis of a Generic Pusher Type Transport Aircraft Configuration in Near-Stall Flight

Amit K Khatri*, Vineet Kumar*
*** CSIR-National Aerospace Laboratories, Bangalore-560017, India**
Keywords: *Bifurcation Analysis, Pusher Type Aircraft, Near-stall flight*

Abstract

Near stall flight of a transport aircraft is many-a-times associated with loss of control problems. A transport aircraft flying inadvertently near stall can rapidly get into upset condition leading to loss of control of aircraft. A systematic investigation of near stall flight characteristics of a transport aircraft, therefore, becomes crucial for ensuring safe flight operation of the aircraft. This paper deals with the detailed investigation of nonlinear flight dynamics of a generic pusher type T-tail transport aircraft configuration in near stall flight regime with the objective of computing safe flight envelope of the aircraft. To the best knowledge of the authors, this is the first ever attempt to study nonlinear flight dynamics of a pusher type T-tail transport aircraft.

1 Introduction

High angle of attack (AOA) aerodynamics of an aircraft is dominated by flow phenomena such as separation, aerodynamic hysteresis effects and vortex breakdown. As a result, high AOA aerodynamics is extremely nonlinear leading to complex flight motions, like wing rock, autorotation, pitch-bucking, deep-stall, spin, etc. High AOA flight near stall is particularly known to be prone to loss of control (LOC) incidents in transport airplanes. A transport aircraft flying inadvertently near stall can quickly get into *upset* condition resulting in loss of control. Considering the increased frequency of aircraft accidents due to LOC, NASA has lately initiated major research programs for systematic investigation of high AOA flight dynamics of transport airplanes [1, 2]. Kwatny et al. [3] analyzed LOC problem for an aircraft model using bifurcation analysis and continuation technique. NASA's generic transport model (GTM), which is representative of a large commercial transport airplane, was taken in their investigation. Bifurcation analysis of the GTM was carried out to determine control strategies required to safely regulate the aircraft near stall bifurcation point so as to avoid LOC. Gill et al. [4] investigated nonlinear dynamics of the GTM model in high AOA flight regime. Bifurcation analysis was performed to identify various attractors that could induce upset condition. It was shown that an inappropriate pilot input can cause the aircraft to enter into an oscillatory spin motion. Chongvisal et al. [5] designed a simple flight control system for prediction and prevention of LOC in an aircraft. The flight control system forewarns of any probable pilot input that can result in LOC during flight. Furthermore, the flight control system provides corrective command inputs to recover back the aircraft from upset condition to safe flying operation mode thereby preventing LOC.

In this paper, we present a detailed analysis of the nonlinear flight dynamics of a generic pusher type T-tail transport aircraft in near-stall flight regime. The paper is organized as follows. Section 2 provides the aerodynamic data for the pusher type transport aircraft model. Section 3 gives a brief introduction to bifurcation analysis and continuation technique. Bifurcation analysis results for the transport aircraft model are presented in section 4. Finally, section 5 concludes the work presented in this paper.

2 Aerodynamic Data for the Aircraft Model

The aircraft model considered in this work is a low wing design with twin engines mounted on rear fuselage via stub wings in pusher type configuration. Empennage is designed as a T-tail layout with horizontal tail atop the vertical stabilizer. The configuration is provided with three primary controls: elevator, aileron and rudder. The configuration is designed for operation at low subsonic Mach numbers (M<0.5).

Extensive wind tunnel tests have been conducted for characterizing aerodynamic behaviour of the aircraft configuration. The aircraft model has been tested for AOA range of -10 to +20 deg and sideslip angles up to +10 deg. A comprehensive aerodynamic database is prepared from the experimental results obtained from wind tunnel tests. Figures 1-4 depict longitudinal and lateral-directional aerodynamic characteristics of the aircraft model. Figure 1 shows lift coefficient (C_L) for the aircraft model; stall AOA for the aircraft can be noted to be around 15 deg. Figure 2 shows the variation in aerodynamic pitching moment coefficient (C_m) at three different sideslip angles. There is a considerable change in pitching moment at 10 deg sideslip angle, though the static longitudinal stability (C_{m_α}) of the aircraft model remains almost unchanged with sideslip. Further, it is observed that the aircraft model loses static longitudinal stability beyond 17 deg AOA. Rolling moment coefficient (C_l) and yawing moment coefficient (C_n) variation with sideslip are presented in Figs. 3 and 4, respectively. The configuration retains lateral stability (C_{l_β}) and directional stability (C_{n_β}) up to AOA 20 deg. However, the configuration is prone to enter into a roll in post-stall flight regime. Strong nonlinearity in pitching, rolling and yawing moment coefficients can be noticed near stall AOA from Figs. 2-4.

Figures 5-7 present control effectiveness of elevator, rudder and aileron, respectively. Pitching moment coefficient for three different elevator settings (neutral, maximum nose-up and maximum nose-down) is shown in Fig. 5.

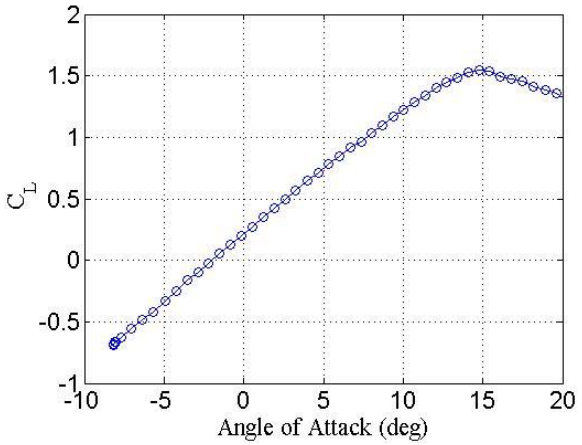

Fig. 1. Plot of lift coefficient against AOA.

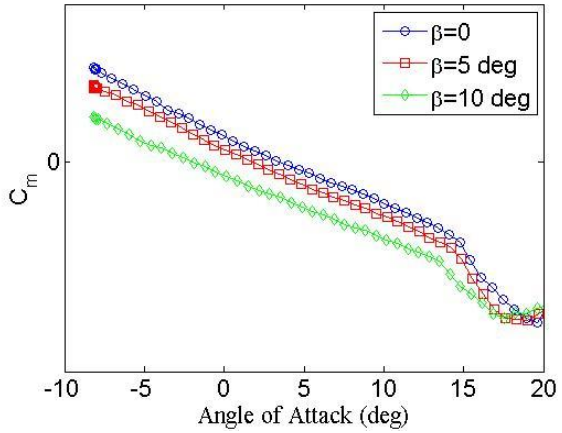

Fig. 2. Plot of pitching moment coefficient against AOA.

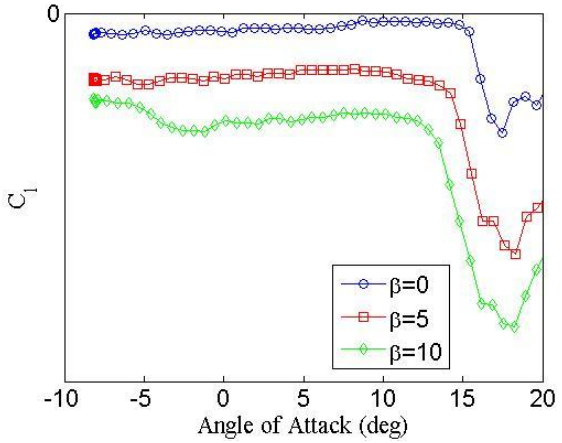

Fig. 3. Plot of rolling moment coefficient versus AOA

Figure 6 shows rudder effectiveness at various AOA for two distinct rudder deflections (neutral and maximum right). Maximum rudder effectiveness is seen to slightly reduce with increase in AOA. Variation in aileron effectiveness with AOA is presented in Fig. 7. A significant reduction in aileron effectiveness

near stall is clearly apparent from Fig. 7 at large aileron deflections.

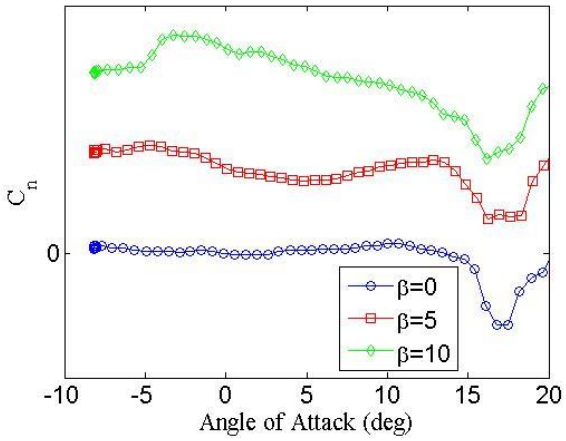

Fig. 4. Plot of yawing moment coefficient versus AOA.

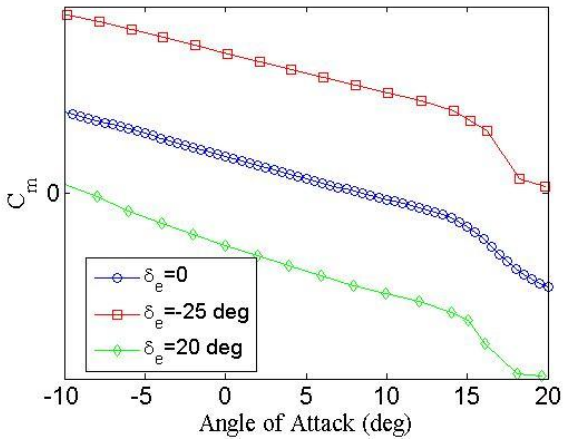

Fig. 5. Plot of pitching moment coefficient versus AOA at different elevator settings.

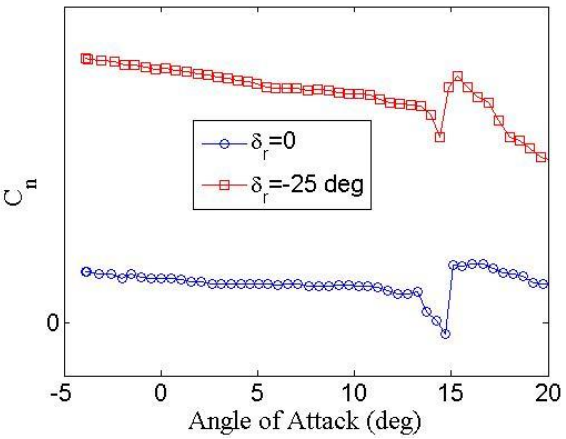

Fig. 6. Plot of yawing moment coefficient versus AOA at different rudder settings.

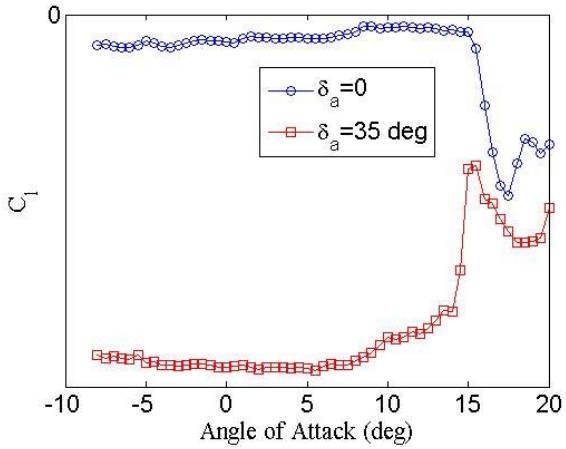

Fig. 7. Plot of rolling moment coefficient versus AOA at different aileron settings $(\delta_a = \delta_{a\_left} + \delta_{a\_right})$.

3 Bifurcation Analysis and Continuation Technique

Bifurcation analysis and continuation technique is a methodology for studying global dynamics of a nonlinear system. Bifurcation analysis of a nonlinear system involves studying changes in plant dynamics as one or more of the system parameters are varied within specified limits. Consider an autonomous nonlinear dynamical system:

$$\dot{\mathbf{x}} = \mathbf{f}(\mathbf{x}, \mathbf{U}) \qquad (1)$$

where $\mathbf{x} \in \Re^n$ is the vector of state variables and vector $\mathbf{U} \in \Re^m$ represents the system parameters. The vector function $\mathbf{f}(\mathbf{x}, \mathbf{U})$ is smooth and defines a mapping: $\Re^n \times \Re^m \to \Re^n$. Bifurcation analysis of a system starts with computing all possible steady state solutions of Eq. (1) for various values of system parameters. In the standard bifurcation analysis (SBA) procedure, only one of the system parameters is varied at a time keeping the remaining parameters as constant. Thus, we solve:

$$\dot{\mathbf{x}} = \mathbf{f}(\mathbf{x}, u, \mathbf{p}) \qquad (2)$$

where u is the continuation parameter and vector $\mathbf{p}$ refers to fixed parameters of the system.

Steady state solutions ($\dot{\mathbf{x}} = \mathbf{0}$) of a nonlinear system can either be equilibrium point or periodic solution. Again, bifurcation in a system indicates a change in either the number of possible steady state solutions or their stability. Bifurcation of an equilibrium point can be static or dynamic. A static bifurcation occurs when a real eigenvalue of the system crosses the imaginary axis. A dynamic or Hopf bifurcation results due to movement of a complex conjugate pair of eigenvalues across the imaginary axis. Hopf bifurcation in a system gives rise to limit cycles, which are isolated closed orbits. Bifurcation of periodic solution is related to the movement of Floquet multiplier across the imaginary axis. Detailed account of bifurcation theory is available in various references [6, 7].

Bifurcation analysis of a nonlinear system is performed with the help of a numerical continuation algorithm. Results from bifurcation analysis are presented in the form of bifurcation diagrams. Various symbols on a bifurcation diagram denote the following:

——————— (solid line) Stable trim point
---------- (dotted line) Unstable trim point
■ Hopf bifurcation point

In this work, AUTO 2000 [8] bifurcation and continuation algorithm is used to carry out the bifurcation analysis. The algorithm computes different steady state solution branches with variation in continuation parameter. Additionally, eigenvalues of the locally linearized system are computed that define stability of the steady state solutions. Different types of bifurcations of equilibrium points and periodic solutions are also indicated by AUTO 2000. Hence, a global dynamical picture of the nonlinear aircraft model can be obtained through AUTO 2000.

3.1 Extended Bifurcation Analysis Method

In the SBA method, only one of the system parameters is varied at a time. This makes the SBA method unsuitable for analyzing constrained nonlinear systems where several control parameters need to be simultaneously varied to satisfy the desired constraints.

The extended bifurcation analysis (EBA) [9] method is a technique for bifurcation analysis of constrained nonlinear system. The EBA method consists of two steps. In step 1 of the EBA method, one solves:

$$\dot{\mathbf{x}} = \mathbf{f}(\mathbf{x}, u, \mathbf{p}) \tag{3}$$

$$\mathbf{g}(\mathbf{x}) = \mathbf{0} \tag{4}$$

where $\mathbf{x} \in \Re^n$ is the state vector, scalar u is the continuation parameter, and vector $\mathbf{p} \in \Re^m$ represents the control parameters. Vector function $\mathbf{g}(\mathbf{x}) \in \Re^k$ refers to the system constraints. To solve the augmented system (3-4), a number of control parameters (equal to k) from vector $\mathbf{p}$ are freed and the remaining parameters are held fixed. It is therefore imperative that the number of control parameters in $\mathbf{p}$ should at least be equal to the number of prescribed constraints (i.e. $m \geq k$). Further, the free control effectors must influence the specified constraints. Solution of step 1 of the EBA method provides steady state solutions satisfying the constraints (4). However, stability of the computed stability solutions is incorrect because constraints are explicitly present in this step.

In step 2 of the EBA method, one solves:

$$\dot{\mathbf{x}} = \mathbf{f}(\mathbf{x}, u, \mathbf{p}_1(u), \mathbf{p}_2) \tag{5}$$

where $\mathbf{p}_1(u)$ are parameter schedules for free parameters as obtained from step 1, and $\mathbf{p}_2$ are fixed control parameters. Output of step 2 gives steady state solutions satisfying the desired constraints (4), along with correct stability information. Besides, bifurcation or departure, if any, from constrained flight conditions are also indicated by this step.

4 Bifurcation Analysis of the Transport Aircraft Model

Application of bifurcation analysis technique to aircraft flight dynamics was first demonstrated by Carroll and Mehra [10]. They showed that various complex high AOA flight dynamical

phenomena exhibited by aircraft are essentially manifestations of different types of bifurcations. Later, Zagyanov and Goman [11] applied bifurcation analysis technique for studying aircraft spin. Over the last three decades bifurcation analysis technique has been widely applied for investigations of high AOA flight dynamics of different aircraft [12, 13].

In this section, we employ the SBA and the EBA method to examine flight dynamics of the pusher type transport aircraft model in different flight conditions. A six degree-of-freedom nonlinear flight dynamic model of the aircraft is used for bifurcation analysis. The flight dynamic model can be represented by a set of nonlinear ordinary differential equations as given in the Appendix. The six aerodynamic coefficients ($C_L, C_D, C_Y, C_l, C_m, C_n$) appearing in the flight dynamic model are computed as below:

$$C_L = C_L(\alpha) + \Delta C_L(\delta_e) + C_{L_q}\frac{q\bar{c}}{2V} \tag{6}$$

$$C_D = C_D(\alpha) + \Delta C_D(\beta) + \Delta C_D(\delta_e) + \Delta C_D(\delta_a) + \Delta C_D(\delta_r) + C_{D_q}\frac{q\bar{c}}{2V} \tag{7}$$

$$C_m = C_m(\alpha) + \Delta C_m(\beta) + \Delta C_m(\delta_e) + C_{m_q}\frac{q\bar{c}}{2V} \tag{8}$$

$$C_Y = C_Y(\alpha) + \Delta C_Y(\beta) + \Delta C_Y(\delta_a) + \Delta C_Y(\delta_r) + C_{Y_p}\frac{pb}{2V} + C_{Y_r}\frac{rb}{2V} \tag{9}$$

$$C_l = C_l(\alpha) + \Delta C_l(\beta) + \Delta C_l(\delta_a) + \Delta C_l(\delta_r) + C_{l_p}\frac{pb}{2V} + C_{l_r}\frac{rb}{2V} \tag{10}$$

$$C_n = C_n(\alpha) + \Delta C_n(\beta) + \Delta C_n(\delta_a) + \Delta C_n(\delta_r) + C_{n_p}\frac{pb}{2V} + C_{n_r}\frac{rb}{2V} \tag{11}$$

where V is the velocity of aircraft; α, β are AOA and sideslip angles, respectively; p, q, r are roll, pitch and yaw rates, respectively; $\delta_e, \delta_a, \delta_r$ refer to elevator, aileron and rudder deflections, respectively. Symbols b and $\bar{c}$ are aircraft span and mean aerodynamic chord, respectively. Symbol $\Delta C_i(j)$ represents the incremental change in parameter C_i due to variation in state variable j.

In this section, we perform constrained bifurcation analysis of the aircraft in straight and level symmetric flight condition. Standard bifurcation analysis of the aircraft near stall is later carried out to examine aircraft behavior near stall. Results for the two cases are presented next.

4.1 Bifurcation Analysis in Level Flight Condition

To perform bifurcation analysis of the aircraft in level flight condition, the EBA method is used to solve the following constrained nonlinear system:

$$\dot{\mathbf{x}} = \mathbf{f}(\mathbf{x}, u, \mathbf{p}) \tag{12}$$

$$\beta = \mathbf{0}, \phi = \mathbf{0}, \gamma = \mathbf{0} \tag{13}$$

where $\mathbf{x} = [V, \alpha, \beta, p, q, r, \phi, \theta]^T$ is the state vector; ϕ, θ being the aircraft roll and pitch angles, respectively. Scalar γ is the flight path angle, $u = [\delta_e]$ is the continuation parameter, and $\mathbf{p} = [\eta, \delta_a, \delta_r]$ is the vector of system parameters (η being the normalized engine thrust). Engine thrust parameter η is defined as:

$$\eta = \frac{\text{Actual engine thrust}}{\text{Maximum static engine thrust}}$$

To solve for the augmented system (12-13), all three parameters in vector $\mathbf{p}$ are freed. Next, the second step of the EBA method is solved. Thus,

the following system of nonlinear equations are solved

$$\dot{\mathbf{x}} = \mathbf{f}(\mathbf{x}, u, \mathbf{p}_1(u), \mathbf{p}_2) \qquad (14)$$

where $\mathbf{p}_1(u) = [\eta(u), \delta_a(u), \delta_r(u)]$ is the vector of free parameters. There are no fixed parameters in this case.

Bifurcation analysis results for the aircraft are shown in Figs. 8-17. Figures 8-10 show schedules for the free parameters as obtained from the first step of the EBA method. It can be noted from Figs. 8-9 that right aileron and right rudder inputs are required to maintain level flight condition near stall. This happens because the aircraft showed a tendency to enter into a left roll at high AOA near stall (refer Fig. 3). Engine thrust is shown in Fig. 10; minimum value of required thrust is noted at an AOA of 7 deg.

Bifurcation plots for level flight constraints (13) are displayed in Figs. 11-13. It can be noticed from these figures that sideslip, bank angle and flight path angle are restricted to zero throughout the flight envelope considered. Figure 14 shows the bifurcation diagram of AOA against elevator deflection. All the trim points of the aircraft can be noted to be unstable; a Hopf bifurcation point near stall AOA (close to 15 deg.) can be clearly noticed from the figure. Bifurcation diagram of Mach number is shown in Fig. 15. Again, it is evident from eigenvalue plot of Fig. 16 that the instability in level flight condition arises due to divergence of spiral mode; the divergence tendency increases sharply beyond an AOA of 10 deg. Figure 17 shows elevator deflection needed to trim the aircraft at different values of lift coefficient in level flight condition. Significant increase in required elevator input for trimming the aircraft close to stall can be observed from Fig. 17.

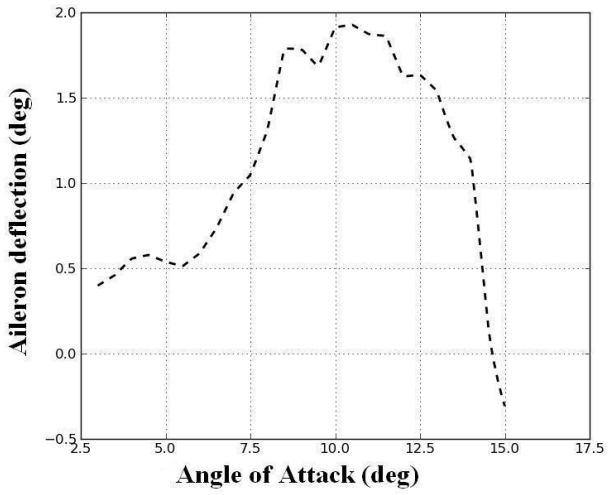

Fig.8. Plot of aileron schedules for level flight.

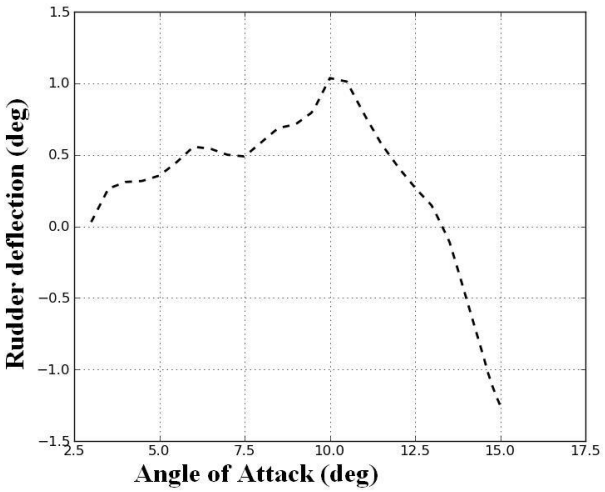

Fig.9. Plot of rudder schedules for level flight.

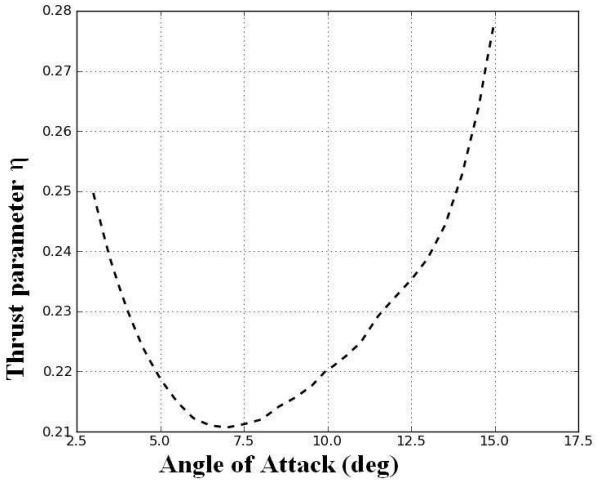

Fig.10. Variation of thrust required at different angle of attack in level flight.

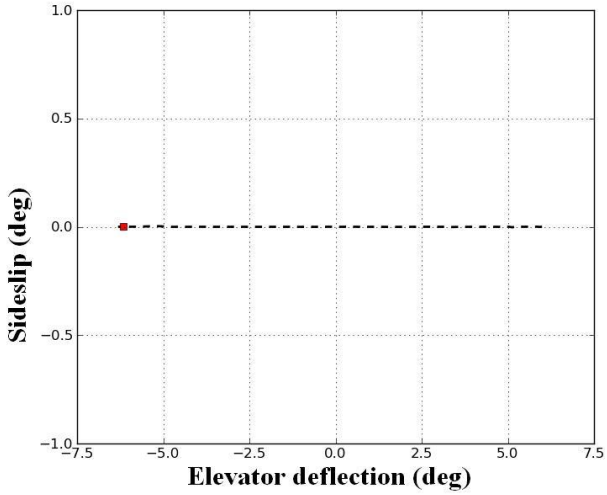

Fig.11. Bifurcation diagram of sideslip against elevator deflection for level flight.

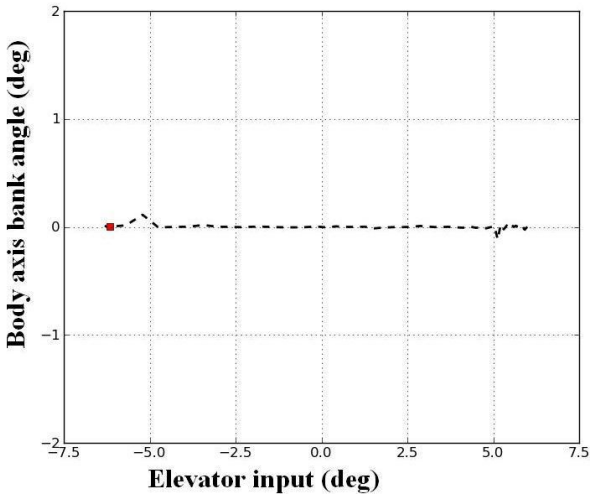

Fig.12. Bifurcation diagram of bank angle against elevator deflection for level flight.

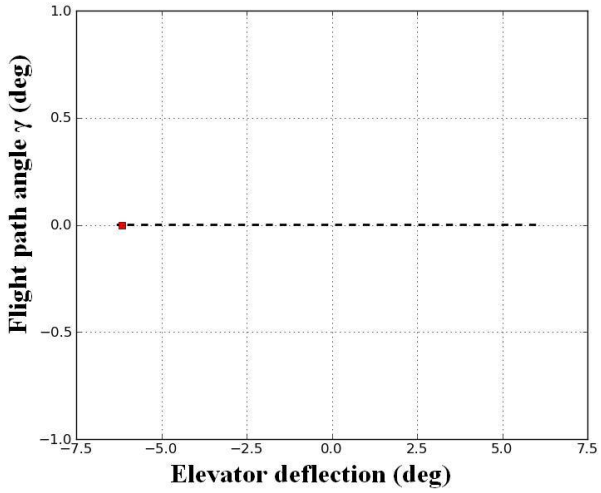

Fig.13. Bifurcation plot of flight path angle against elevator deflection for level flight.

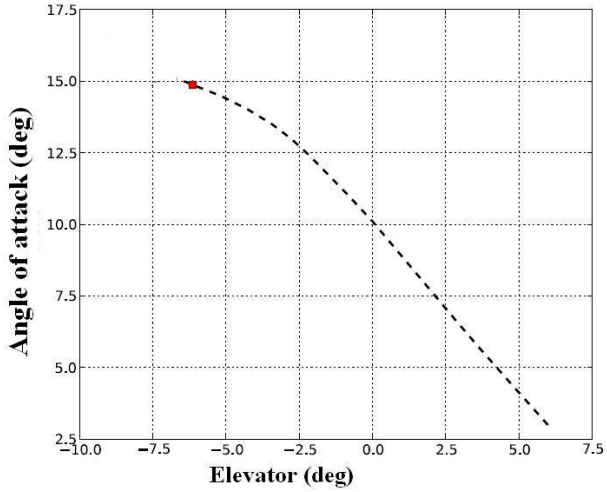

Fig.14. Bifurcation diagram of angle of attack against elevator deflection for level flight.

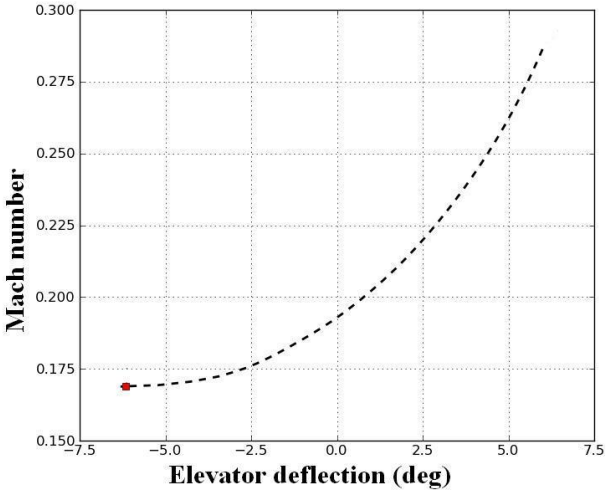

Fig.15. Bifurcation diagram of Mach number against elevator deflection for level flight.

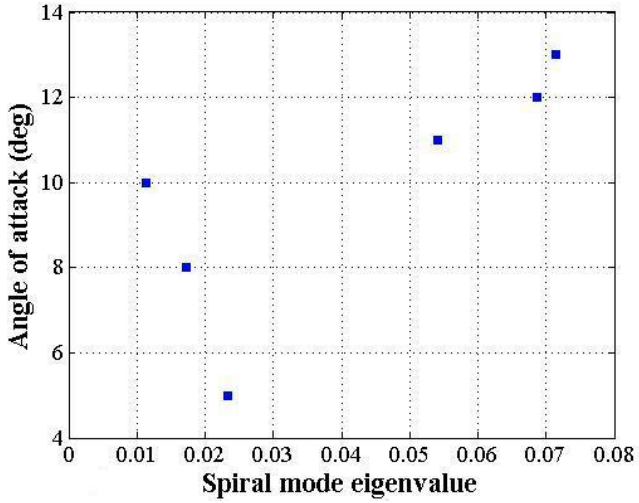

Fig. 16. Variation of spiral mode eigenvalue with angle of attack.

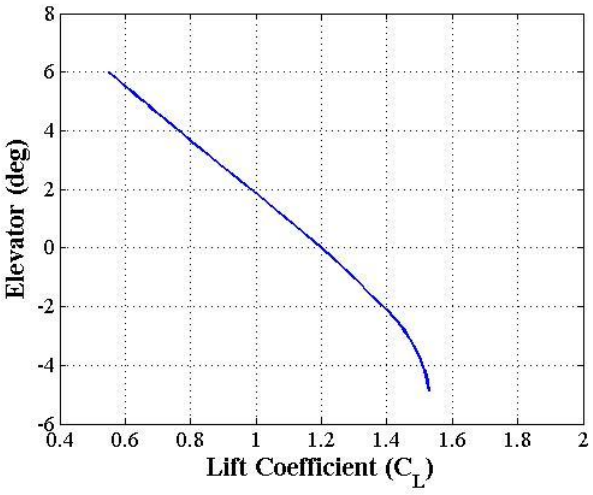

Fig.17. Plot of elevator against lift coefficient (C_L) in level flight condition.

4.2 Bifurcation Analysis of the Aircraft near Stall-α

Stall of an aircraft is a mandatory flight test to be done for showing compliance with the certification requirements. As the aircraft aerodynamics is highly nonlinear near stall, a thorough study of the aircraft behavior close to stall is needed to investigate any tendency of the aircraft to depart into uncontrolled flight motion. In this section, we analyse the aircraft dynamics near stall to assess aircraft response while approaching stall.

To perform nonlinear analysis of the aircraft near stall, starting point for bifurcation analysis procedure is taken as level flight trim point at AOA 13 deg. The corresponding state and control vectors for this initial point are available from bifurcation analysis results of the previous subsection 4.1. Standard bifurcation analysis procedure is carried out to solve the following system of equations:

$$\dot{\mathbf{x}} = \mathbf{f}(\mathbf{x}, u, \mathbf{p}) \qquad (15)$$

where $\mathbf{x} = [V, \alpha, \beta, p, q, r, \phi, \theta]^T$ is the state vector; $u = [\delta_e]$ is the continuation parameter; and $\mathbf{p} = [\eta, \delta_a, \delta_r]$ is the vector of fixed system parameters.

Bifurcation analysis results obtained from standard bifurcation analysis of the system (15) are provided in Figs. 18-23. Figure 18 shows bifurcation plot of AOA versus continuation parameter δe. The maximum attainable AOA is 14.6 deg at $\delta e = -7$ deg. No steady state solutions exist beyond an elevator deflection of -7 deg in this case. A saddle node bifurcation occurs at AOA 14.6 deg. All the steady state solutions on upper branch are unstable; a small region of stable solutions is seen on lower branch between AOA range of 12-13 deg. The stable solution branch exists for $-3 \le \delta_e \le -4$ deg. Three Hopf bifurcation points are visible at AOA of 12 deg, 13 deg and 14.6 deg. Bifurcation diagrams of sideslip and bank angle are shown in Figs. 19 and 20, respectively. Bank angle on the stable branch is

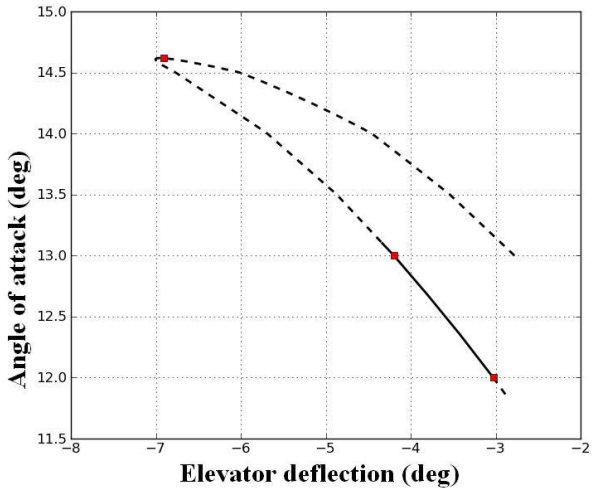

Fig.18. Bifurcation diagram of angle of attack against elevator deflection.

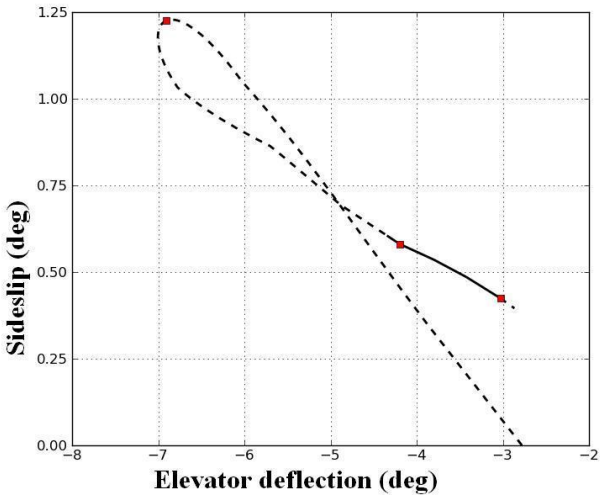

Fig.19. Bifurcation diagram of sideslip.

quite large (~70 deg). Bifurcation plots for roll rate, pitch rate and yaw rate are provided in Figs. 21, 22 and 23, respectively. It can be concluded from the bifurcation analysis results that the aircraft has a tendency to enter into a right roll during stall. Because all the solutions near stall are unstable, a significant amount of effort will be required on the part of pilot to prevent spiral divergence while approaching stall.

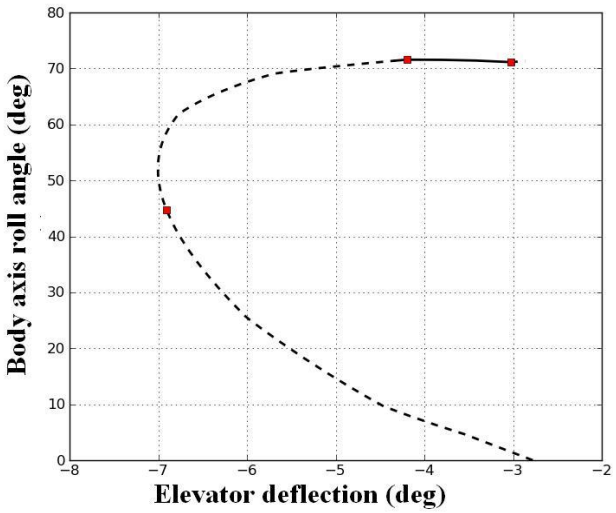

Fig.20. Bifurcation diagram of bank angle.

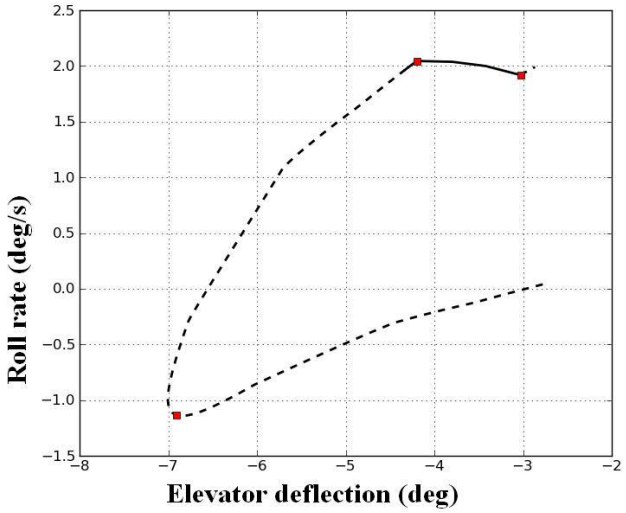

Fig.21. Bifurcation plot of aircraft roll rate.

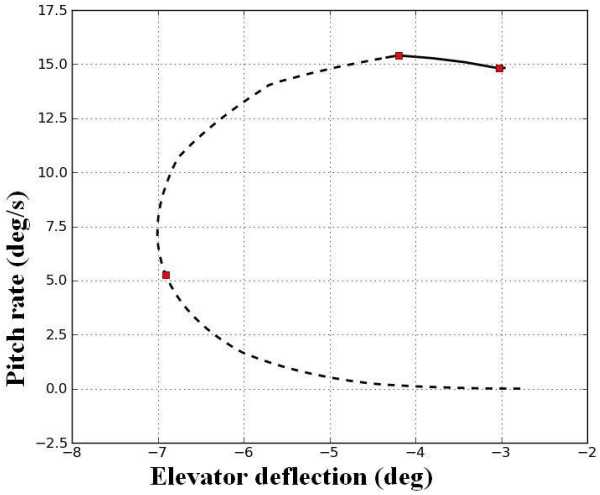

Fig.22. Bifurcation plot of aircraft pitch rate.

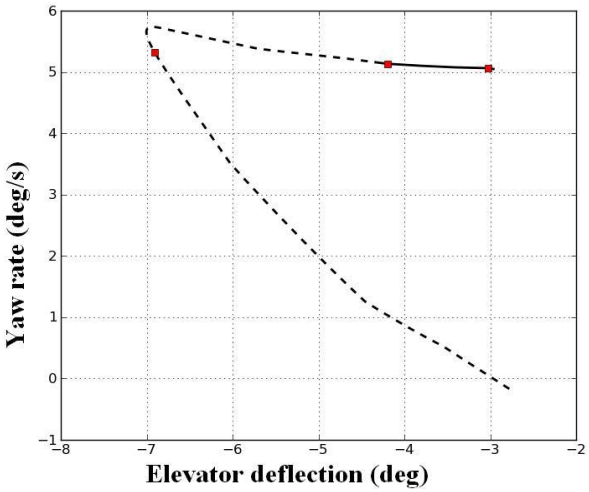

Fig.23. Bifurcation plot of aircraft yaw rate.

5 Conclusions

Nonlinear analysis of a pusher type T-tail transport aircraft configuration has been presented in this paper. Bifurcation analysis and continuation methodology is adopted for nonlinear flight dynamics analysis of the aircraft. Bifurcation analysis results for the aircraft in level flight condition reveal that the aircraft is unstable in spiral mode throughout its flight envelope. Further, the aircraft is likely to enter into a roll on approaching stall. Nonlinear dynamic analysis for the aircraft discussed in this paper has however been limited to studying the effect of variation in elevator control. Bifurcation analysis with respect to aileron and rudder controls needs to be further carried out to

fully characterize the aircraft dynamics near stall. This forms a part of future work and is currently under investigation.

Appendix: Equations of motion

$$\dot{V} = \frac{1}{m}\left[T_m \eta \cos\alpha \cos\beta - \frac{1}{2}\rho V^2 S C_D - mg \sin\gamma\right]$$

$$\dot{\alpha} = q - \frac{1}{\cos\beta}[(p\cos\alpha + r\sin\alpha)\sin\beta$$

$$+\frac{1}{mV}\{T_m \eta \sin\alpha + \frac{1}{2}\rho V^2 S C_L$$

$$-mg\cos\mu\cos\gamma\}]$$

$$\dot{\beta} = \frac{1}{mV}[-T_m \eta \cos\alpha \sin\beta$$

$$+\frac{1}{2}\rho V^2 S C_Y + mg\sin\mu\cos\gamma] + (p\sin\alpha - r\cos\alpha)$$

$$\dot{p} = \frac{I_y - I_z}{I_x} qr + \frac{1}{2I_x}\rho V^2 S b C_l$$

$$\dot{q} = \frac{I_z - I_x}{I_y} pr + \frac{1}{2I_y}\rho V^2 S \bar{c} C_m$$

$$\dot{r} = \frac{I_x - I_y}{I_z} pq + \frac{1}{2I_z}\rho V^2 S b C_n$$

$$\dot{\phi} = p + q\sin\phi\tan\theta + r\cos\phi\tan\theta$$

$$\dot{\theta} = q\cos\phi - r\sin\phi$$

$$\dot{\psi} = \frac{q\sin\phi + r\cos\phi}{\cos\theta}$$

Wind axis Euler angles (μ, γ) and body axis Euler angles (ϕ, θ) are related by the following kinematic relations:

$$\sin\gamma = \cos\alpha\cos\beta\sin\theta - \sin\beta\sin\phi\cos\theta$$

$$-\sin\alpha\cos\beta\cos\phi\cos\theta$$

$$\sin\mu\cos\gamma = \cos\alpha\sin\beta\sin\theta + \cos\beta\sin\phi\cos\theta$$

$$-\sin\alpha\sin\beta\cos\phi\cos\theta$$

$$\cos\mu\cos\gamma = \sin\alpha\sin\theta + \cos\alpha\cos\phi\cos\theta$$

References

[1] Foster, J. V., Cunningham, K., Fremaux, C. M., Shah, G. H., Stewart, E. C., Rivers, R. A., Wilborn, J. E., and Gato, W.,"Dynamics Modeling and Simulation of Large Transport Airplanes in Upset Conditions," *Proc. AIAA Guidance, Navigation, and Control Conference*, California, AIAA paper 2005-5933, 2005.

[2] Belcastro, C. M., Newman, R. L., Crider, D. A., Groff, L., Foster, J. V., and Klyde, D. H., "Preliminary Analysis of Aircraft Loss of Control Accidents: Worst Case Precursor Combinations and Temporal Sequencing," *AIAA Guidance, Navigation, and Control Conference*, Maryland, AIAA paper 2014-0612, 2014.

[3] Kwatny, H. G., Dongmo, J. T., Chang, B., Bajpai, G., Yasar, M., and Belcastro, C., "Nonlinear analysis of aircraft loss of control," *Journal of Guidance Control and Dynamics*, Vol. 36, No. 1, pp. 149–162, 2013.

[4] Gill, S. J., Lowenberg, M. H., Neild, S. A., Krauskopf, B., Puyou, G., and Coetzee, E., "Upset Dynamics of an Airliner Model: A Nonlinear bifurcation Analysis," *Journal of Aircraft*, Vol. 50, No.6, pp. 1832–1842, 2013.

[5] Chongvisal, J., Nikolas, T., Xargay, E., Talleur, D. A., Kirlik, A., and Hovakimyan, N., "Loss-of-Control Prediction and Prevention for NASA's Transport Class Model," *Proc. AIAA Guidance, Navigation, and Control Conference*, Maryland, AIAA paper 2014-0784, 2014.

[6] Strogatz, S., *Nonlinear Dynamics and Chaos*, Addison Wesley Longman, Reading, MA, 1994.

[7] Kuznetsov, Y. A., *Elements of Applied Bifurcation Theory*, Springer, New York, 2004.

[8] Doedel, E. J., Paffenroth, R. C., Champneys, A. R., Fairgrieve, T. F., Kuznetsov, Y. A., Oldeman, B. E., Sandstede, B., and Wang, X., "AUTO2000: Continuation and Bifurcation Software for Ordinary Differential Equations (with HomCont)," California Inst. of Technology, Technical Rept., Pasadena, 2001.

[9] Ananthkrishnan, N., and Sinha, N. K., "Level Flight Trim and Stability Analysis using Extended Bifurcation and Continuation Procedure," *Journal of Guidance, Control, and Dynamics*, Vol. 24, No. 6, 2001, pp. 1225-1228.

[10] Carroll, J. V., and Mehra, R. K., "Bifurcation Analysis of Nonlinear Aircraft Dynamics," *Journal of Guidance, Control, and Dynamics*, Vol. 5, No. 5, pp. 529–536, 1982.

[11] Zagaynov, G. I., and Goman, M. G., "Bifurcation analysis of critical aircraft flight regimes," ICAS paper 84-4.2.1, 1984.

[12] Goman, M. G., Zagaynov, G. I., and Khramtsovsky, A. V., "Application of Bifurcation Methods to Nonlinear Flight Dynamics Problems," *Progress in*

Aerospace Sciences, Vol. 33, No. 9–10, pp. 539–586, 1997.

[13] Paranjape, A., Sinha, N. K., and Ananthkrishnan, N., "Use of Bifurcation and Continuation Methods for Aircraft Trim and Stability Analysis- A State-Of-The-Art," *Journal of Aerospace Sciences and Technologies*, Vol. 60, No. 2, 2008.

Contact Author Email Address

Mail to: khatri@ccadd.cmmacs.ernet.in, kvineet@ccadd.cmmacs.ernet.in

Copyright Statement